Complementary apodized grating waveguides for tunable optical delay lines

Saeed Khan[1, 2] and Sasan Fathpour[1,2,*]

[1]*CREOL, The College of Optics and Photonics, University of Central Florida, Orlando, FL 32816 USA*
[2]*Department of Electrical Engineering and Computer Science, University of Central Florida, Orlando, FL 32816 USA*
[*]*fathpour@creol.ucf.edu*

Abstract: A novel class of high-speed and tunable integrated photonic delay lines that compromise between loss and size is proposed. The devices consist of two cascaded apodized grating waveguides and with complementary (positively and negatively modulated) refractive index profiles for dispersion compensation. It is shown that the compact tunable delay lines are low-loss and offer long true-time delays and tuning ranges and high operation bit rates.

OCIS codes: (250.0250) Optoelectronics; (250.5300) Photonic integrated circuit.

References and links

1. S. Yegnanarayanan, P. D. Trinh, F. Coppinger, and B. Jalali, "Compact silicon-based integrated optic time delays," IEEE Photon. Technol. Lett. **9**(5), 634–635 (1997).
2. A. Yariv, Y. Xu, R. K. Lee, and A. Scherer, "Coupled-resonator optical waveguide: A proposal and analysis," Opt. Lett. **24**(11), 711–713 (1999).
3. F. Xia, L. Sekaric, and Y. Vlasov, "Ultracompact optical buffers on a silicon chip," Nat. Photonics **1**(1), 65–71 (2007).
4. F. Morichetti, A. Melloni, C. Ferrari, and M. Martinelli, "Error-free continuously-tunable delay at 10 Gbit/s in a reconfigurable on-chip delay-line," Opt. Express **16**(12), 8395–8405 (2008).
5. A. Melloni, A. Canciamilla, C. Ferrari, F. Morichetti, L. O'Faolain, T. F. Krauss, R. De La Rue, A. Samarelli, and M. Sorel, "Tunable delay lines in silicon photonics: coupled resonators and photonic crystals, a comparison," IEEE Photon. J. **2**(2), 181–194 (2010).
6. J. Cardenas, M. A. Foster, N. Sherwood-Droz, C. B. Poitras, H. L. R. Lira, B. Zhang, A. L. Gaeta, J. B. Khurgin, P. Morton, and M. Lipson, "Wide-bandwidth continuously tunable optical delay line using silicon microring resonators," Opt. Express **18**(25), 26525–26534 (2010).
7. J. Adachi, N. Ishikura, H. Sasaki, and T. Baba, "Wide range tuning of slow light pulse in SOI photonic crystal coupled waveguide via folded chirping," IEEE J. Sel. Top. Quantum Electron. **16**(1), 192–199 (2010).
8. B. Jalali and S. Fathpour, "Silicon photonics," J. Lightwave Technol. **24**(12), 4600–4615 (2006).
9. J. E. Sipe, L. Poladian, and C. M. de Sterke, "Propagation through nonuniform grating structures," J. Opt. Soc. Am. A **11**(4), 1307–1320 (1994).
10. J. B. Khurgin, J. U. Kang, and Y. J. Ding, "Ultrabroad-bandwidth electro-optic modulator based on a cascaded Bragg grating," Opt. Lett. **25**(1), 70–72 (2000).
11. J. B. Khurgin and P. A. Morton, "Tunable wideband optical delay line based on balanced coupled resonator structures," Opt. Lett. **34**(17), 2655–2657 (2009).
12. S. Khan, M. A. Baghban, and S. Fathpour, "Electronically tunable silicon photonic delay lines," Opt. Express **19**(12), 11780–11785 (2011).
13. S. G. Johnson, M. L. Povinelli, M. Soljacic, A. Karalis, S. Jacobs, and J. D. Joannopoulos, "Roughness losses and volume-current methods in photonic-crystal waveguides," Appl. Phys. B **81**(2–3), 283–293 (2005).
14. I. Giuntoni, D. Stolarek, A. Gajda, J. Bruns, L. Zimmermann, B. Tillack, and K. Petermann, "Integrated drop-filter for dispersion compensation based on SOI rib waveguides" in 37th European Conference and Exhibition on Optical Communication (ECOC), p. Th.12.LeSaleve.4 (2011).
15. P. Yeh, *Optical Waves in Layered Media* (Wiley, 1988), p. 102.
16. G. P. Agrawal, *Fiber-Optic Communication Systems* (Wiley, 2002), p. 26.
17. T. Erdogan, "Fiber grating spectra," J. Lightwave Technol. **15**(8), 1277–1294 (1997).
18. Y. A. Vlasov, M. O'Boyle, H. F. Hamann, and S. J. McNab, "Active control of slow light on a chip with photonic crystal waveguides," Nature **438**(7064), 65–69 (2005).
19. P. Dong, W. Qian, S. Liao, H. Liang, C. C. Kung, N. N. Feng, R. Shafiiha, J. Fong, D. Feng, A. V. Krishnamoorthy, and M. Asghari, "Low loss shallow-ridge silicon waveguides," Opt. Express **18**(14), 14474–14479 (2010).

#168100 - $15.00 USD Received 17 May 2012; revised 4 Aug 2012; accepted 5 Aug 2012; published 15 Aug 2012

1. Introduction

Tunable optical true-time delay lines are key components in a host of photonic and electronic-photonic systems. Among other material systems, silicon-based waveguides have been long reported to reduce the footprint of integrated delay lines as compared with optical fiber-based solutions [1]. Group delay can be further enhanced, and the footprint can be significantly reduced, in guided resonant buffers [2]. All-pass filters (APF) [3], coupled-resonator optical waveguides (CROW) [3–5] and side-coupled integrated spaced sequence of resonators (SCISSOR) [6] are commonly pursued resonator-based schemes. Also, slowing down light in photonic crystal (PhC) line-defect waveguides has been demonstrated [5], [7]. However, in all of these approaches the loss can be very high as compared with spiral waveguides. For instance, in one report on CROWs and APFs, loss per unit delays of 104 and 43 dB/ns were attained, respectively, while submicron bent waveguides had a much less loss of 14 dB/ns [3]. Similarly, PhC devices suffer from high losses (35-100 dB/ns [5], [7]).

Here, a novel class of tunable photonic delay lines is proposed, whose architecture offers a compromised solution between size and loss. The core concept is based on engineering the time delay spectrum of grating waveguides by apodizing the gratings' profiles. More interestingly, cascading complementary (positively and negatively modulated index profile) grating waveguides allows for dispersion compensation in order to achieve very high bit rate operation. Both transmission- and reflection-mode devices can be envisaged. Tuning of the attainable delay time is feasible through thermooptic or electrooptic effects. In principle, the proposed devices may be implemented in any integrated optics technology. In the following, the versatile silicon photonics platform [8] is chosen for proving the concept.

2. Operating principle

Figures 1(a) and 1(b) depict two complementary types of proposed apodized grating waveguide photonic delay lines on the silicon-on-insulator (SOI) platform for transmission mode of operation. In either device type, optical delay is essentially achieved via multiple reflections in the distributed Bragg reflectors. One advantage of using apodized gratings in the present scheme, as compared to PhC waveguides, is that it allows avoiding the complications that were observed in uniform gratings due to group delay ripples in the vicinity of the operation wavelength. Another advantage is that the devices will not suffer from reflection losses, as will be discussed later. Either device type can be individually used as a delay line. However, the overall device performance is significantly enhanced if they are appropriately cascaded.

The device in Fig. 1(a), denoted as type 1, consists of a SOI waveguide with an outward grating profile which is apodized by a super-Gaussian function. The outward grating causes an increase in the grating effective index as the grating width increases. This results in a higher Bragg wavelength for the center of the grating as compared to its wings. Meanwhile, the lower Bragg wavelengths of the end wings form a Fabry-Perot (FP) cavity at wavelengths below the stop-band [9], while the delay spectrum above the stop-band is smooth and decreases with wavelength (normal dispersion). This description is schematically depicted in the transmission delay spectrum of grating 1 in Fig. 1(c). Meanwhile, the type 2 device, shown in Fig. 1(b), has an inward grating and its delay spectrum is almost the mirror image of the type 1 device (Fig. 1(c)), i.e., it has anomalous dispersion below its grating stop-band.

In either device type, by increasing the effective refractive index of the silicon grating waveguide by thermooptic effect, the whole delay spectrum is red-shifted. The red-shift increases or decreases the delay of the transmitted light depending on whether the normal or the anomalous dispersion of the delay spectrum occurs in the vicinity of the operating wavelength. If the dispersion is anomalous and the incident wavelength is fixed at the highest wavelength value in the tuning range, the delay of the transmitted light will decrease with an increase in the effective index. The opposite is true for the normal dispersion case.

#168100 - $15.00 USD Received 17 May 2012; revised 4 Aug 2012; accepted 5 Aug 2012; published 15 Aug 2012

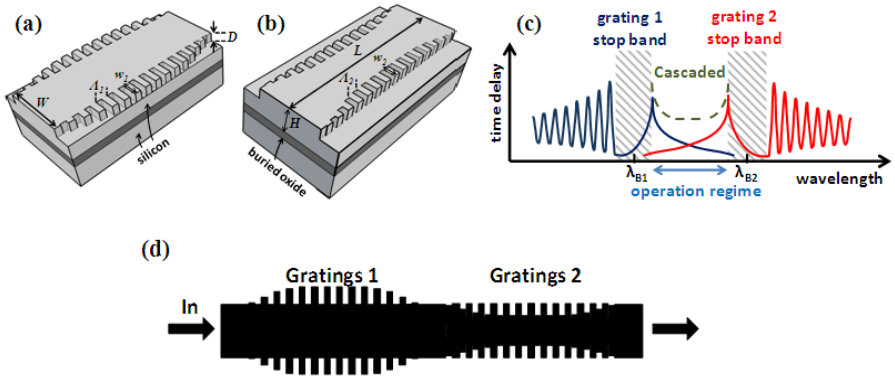

Fig. 1. (a) Type 1 and (b) Type 2 of the proposed transmission-mode complementary grating waveguide delay lines; (c) Working principle of each device type and how cascading them allows dispersion compensation in the shown operation regime; (d) Schematic of how cascading can be achieved for transmission-mode operation.

A very interesting feature of the proposed scheme is that the almost mirror-image delay spectra of the two device types can be taken advantage of for dispersion compensation in order to achieve very high operation bandwidths. Indeed, cascading the complementary grating waveguides (Fig. 1(d)) allows mutual compensation of the gratings' dispersions provided that appropriate center Bragg wavelengths, λ_{B1} and λ_{B2}, are chosen. The schematic shown in Fig. 1(c) suggests that for $\lambda_{B1} < \lambda_{B2}$ a relatively flattened dispersion relation can be obtained in the operation regime of the cascaded device. Consequently, high delay and high bandwidth are simultaneously achievable in the wavelength range between the two stop-bands of the cascaded gratings. This cascading approach has some resemblance to a group-velocity matching technique proposed for $LiNbO_3$ electro-optic modulators [10] and balancing of dispersion in SCISSOR-based delay lines [6,11]. Tuning of the attainable time delay can meanwhile be achieved by either the thermooptic effect via microheaters integrated on top of the waveguides (shown in Fig. 2) or by the electrooptic effect via *p-n* junction diodes [12].

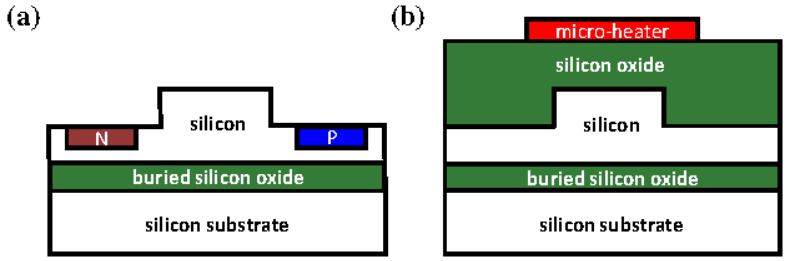

Fig. 2. Schematics showing the cross-section of the waveguide delay line and how the delay can be tuned using (a) electrooptic effect via *p-n* junction diodes and (b) thermooptic effect via micro-heaters.

To avoid group delay ripples in the vicinity of the band edge in the pass-band, it is necessary to apodize the gratings [9]. The super-Gaussian function was recognized as the best profile (compared to linear, Gaussian and raised cosine functions) for apodizing the gratings in the transmission mode. Also, by using super-Gaussian apodization, the gratings transmittivity transitions sharply to almost 100% at the band edge in an ideal device in which the propagation loss is ignored (see Fig. 4(b)). Indeed, without proper apodization, an undesired FP cavity, with considerable reflection loss, is formed between the two complementary gratings in the operation regime. Also, the absence of these FP resonances in apodized gratings implies that the choice of the gap length between the two gratings is not

#168100 - $15.00 USD Received 17 May 2012; revised 4 Aug 2012; accepted 5 Aug 2012; published 15 Aug 2012

important. The gap may be essential to avoid thermal crosstalk between microheaters of the cascaded gratings, as discussed in Section 4. In practice, the gap can be replaced with a folded bent waveguide in order to reduce the total length of the delay chips by about half. Finally, the sharp transition of the transmittivity to about 100% at the band edge (see Fig. 4(b)) allows operation in its proximity, where the highest group delays are achievable with no reflection loss. This is a clear advantage over PhC waveguide delay lines which suffer from high reflection loss close to the band edge [13].

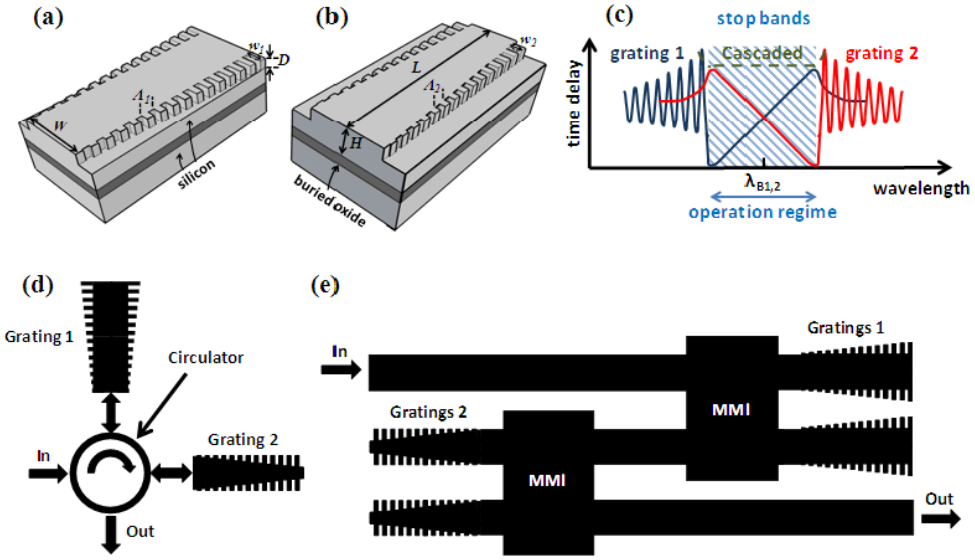

Fig. 3. (a) Type 1 and (b) Type 2 of the proposed reflection mode complementary grating waveguide delay lines with linear grating profiles; (c) Working principle of each reflection mode device and how cascading them allows dispersion compensation in the shown operation regime; Two scheme for cascading reflection mode devices using (a) optical circulators and (e) Multi-mode interferometers.

We have previously proposed and studied the performance of similar devices but operating in the reflection mode using Gaussian apodization profiles and *p-n* junction diodes for tuning the delay [12]. Here, the possibility of cascading two of the devices for higher performance is examined. It turns out that neither Gaussian nor super-Gaussian profiles are the best choice for complementary dispersion relations in the stop band of the gratings that are tuned using the thermooptic effect. Rather, linear grating profiles (Fig. 3(a) and 3(b)) possess close to linear dispersion relations and hence almost dispersion-flat devices are feasible if two such complementary gratings are cascaded (Fig. 3(c)). In practice, cascading of two devices in the reflection mode can be achieved by an optical circulator (Fig. 3(d)). If a monolithically integrated system is desired, four gratings and two multi-mode interferometers (MMIs) can be employed using the arrangement shown in Fig. 3(e), as proposed before for drop filters [14]. Essentially, the two MMIs ought to be designed such that when the optical signal reflects from the linear gratings, the signal is directed towards the output of the shown system.

3. Model

The reflection and transmission coefficients of several structures were calculated and optimized using the standard transfer matrix method [15]. This method was chosen due to its reasonably small computation time. Its validity and accuracy was confirmed by comparing it with the coupled-mode theory for some of the structures. The effective refractive index of each corrugated section was determined using the commercial RSoft simulator. A thermo-optic coefficient of 1.86×10^{-4} K^{-1} was used to determine the thermally-induced refractive

#168100 - $15.00 USD Received 17 May 2012; revised 4 Aug 2012; accepted 5 Aug 2012; published 15 Aug 2012

index change in the silicon structure. Pulse-broadening of transform-limited input pulses were calculated based on the dispersion of the delay lines. The criterion for bit rate estimations was that 95% of the output pulse energy would remain in its corresponding time slot [16].

According to the notations of Figs. 1 and 3, $W = 1.5$ µm, $H = 2$ µm, $D = 1$ µm, $L = 0.5$ cm, $w_1 \approx 250$ nm and $w_2 \approx 160$ nm were used in the design of both transmission- and reflection-mode cascaded devices. The choices of the nonidentical grating periods for operation in the 1,550 nm band were $\Lambda_1 = 224.6$ nm and $\Lambda_2 = 225.9$ nm for transmission-mode devices and slightly different ($\Lambda_1 = 225.0$ nm and $\Lambda_2 = 225.5$ nm) for reflection-mode devices. The full width at half maximum (FWHM) of the employed optimized super-Gaussian function of order 12 was 0.72 cm and 0.8 cm for transmission-mode gratings 1 and 2, respectively. The grating widths of the reflection-mode devices were linearly varied from zero to the mentioned maximum values of w_1 and w_2 for type 1 and 2, respectively. A grating waveguide propagation loss of 1.5 dB/cm [14] was incorporated in the transfer matrix method and in the following results, unless otherwise stated.

4. Results and discussions

Figure 4(a) shows the individual (non-cascaded) transmission and delay spectra of a 1-cm-long type 1 transmission-mode device. An almost mirror-like image is obtained for grating 2 (Fig. 4(b)). The other difference between Figs. 4(a) and 4(b) is that gratings with no propagation loss were assumed in the latter case to emphasize that 100% transmission in the operation regime is ideally possible. In other words, propagation loss is the only loss mechanism in the proposed devices and the gratings' reflection loss is negligible.

When propagation loss is included, both type 1 and type 2 have a tunability bit-rate product of about one and an identical true time delay in the range of 120 to 210 ps. For tunable delay lines, the optimized condition at which the attainable tunability bit-rate product is maximal may be preferred over the delay bit-rate product. For this operating condition, the tunability of the type 1 device is ~90 ps (from 120 to 210 ps). Higher values are attainable for lower propagation loss value. In ideal lossless gratings, the true time delay can be as high as 530 ps and the tunability can be 410 ps.

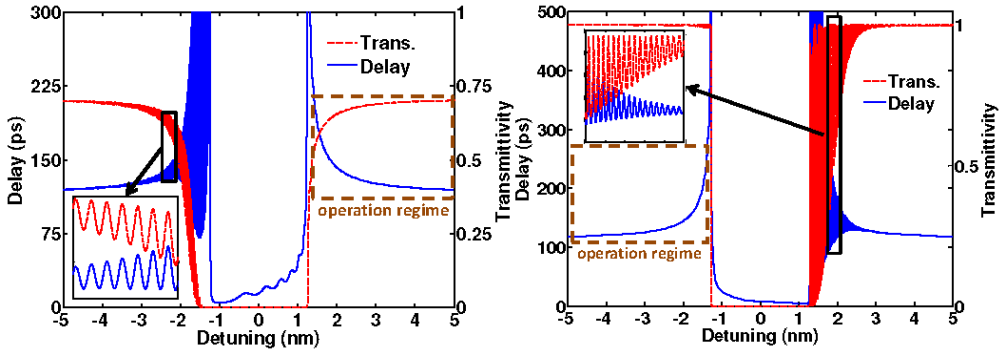

Fig. 4. Transmission and delay spectra of (a) outward and (b) inward apodized gratings using the super-Gaussian function corresponding to gratings 1 and 2 of Fig. 1, respectively. The Bragg wavelength (zero detuning) is at λ_B = 1,550 nm in both cases, that is identical corrugation periods of Λ = 225.2 nm.

It is noted that the apparent oscillatory regions in the delay spectra (the zoomed sections in the insets of Fig. 3) are not used in the present device, and hence are not concerned, in principle. Nonetheless, the oscillations can be totally eliminated by envisioning an index profile that has a zero dc value [17]. Such a zero-dc profile can be practically achieved if both the waveguide and the grating widths, W and w, follow super-Gaussian functions. However, our studies (not presented here) suggest that the performance of such a device is very similar to that of Fig. 1. Meanwhile, designing a zero-dc profile (using four different super-Gaussian

#168100 - $15.00 USD Received 17 May 2012; revised 4 Aug 2012; accepted 5 Aug 2012; published 15 Aug 2012

functions) is more complicated and its operation is expected to be much more sensitive to fabrication errors than the presented case.

Figures 5(a) and 5(b) present the transmission and delay spectra for the transmission-mode cascaded device of Fig. 1(c) and how the spectra can be thermally tuned. The aforementioned corrugation periods were chosen such that the upper stop-band edge of grating 1 (when it is heated to 30°C above room temperature, i.e., $T_1 = R_T + 30°C$) coincides with the lower stop-band edge of grating 2 (when it is kept at R_T), i.e., $\Delta T = T_2 - T_1 = -30°C$. Under these conditions, the time delay is at its maximum and the bit rate is at its minimum. Varying ΔT to ~ + 30°C shifts the device to the other extreme, i.e., minimum delay and maximum bit rate.

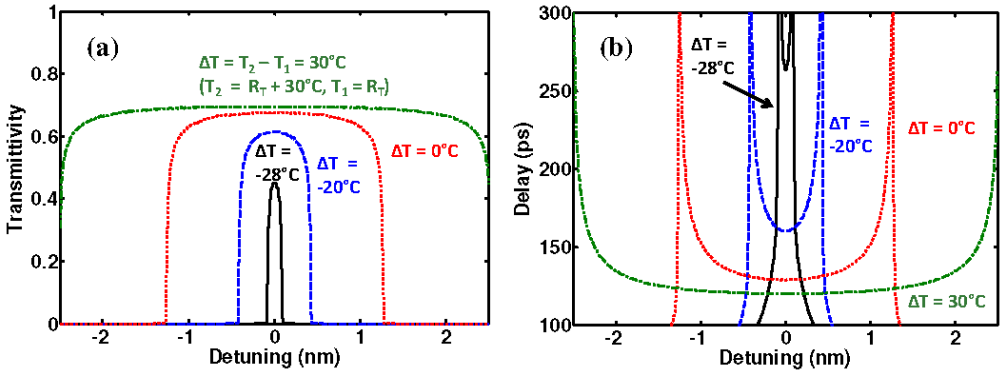

Fig. 5. (a) Transmission and (b) delay spectra of transmission-mode cascaded devices for various $\Delta T = T_2 - T_1$ (temperature difference of grating 1 and grating 2) around a center wavelength of 1,550 nm.

The thermal crosstalk between the cascaded gratings with a temperature difference of up to 30°C can be minimized by inserting a gap between them. To estimate the required gap length, the thermal crosstalk between two cascaded gratings in the transmission mode was calculated using the 3-D heat diffusion module of COMSOL™. The results suggest that a minimum length of 2 μm is necessary to keep the thermal crosstalk < 10%. For a crosstalk of < 1%, the minimum gap length should be 4.4 μm. The gap can be easily incorporated between the two cascaded gratings with no impact on the optical properties of the system because of the absence of FP cavity formation between the gratings, as discussed before.

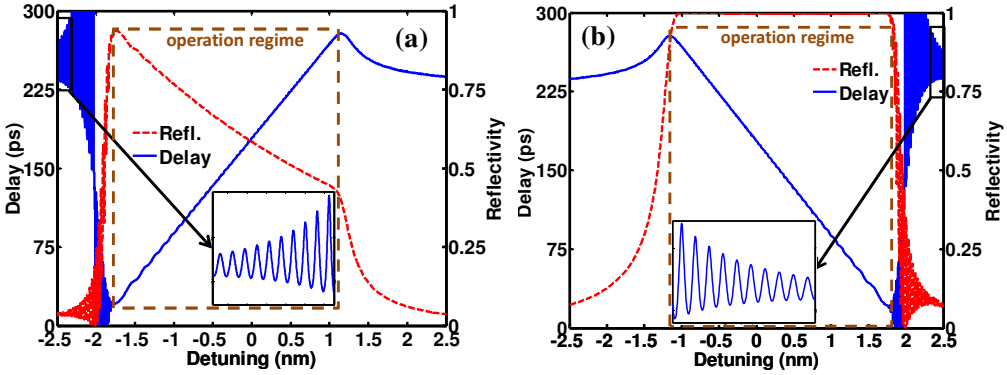

Fig. 6. Reflection and delay spectra of (a) Type 1 reflection-mode device (Fig. 3(a)) and (b) Type 2 reflection mode device (Fig. 3(b)). The Bragg wavelength (zero detuning) is at λ_B = 1,550 nm and the corrugation periods are Λ = 225.2 nm in both devices.

#168100 - $15.00 USD Received 17 May 2012; revised 4 Aug 2012; accepted 5 Aug 2012; published 15 Aug 2012

Figure 6 shows the mirror-like delay and reflection spectra of type 1 and 2 reflection-mode devices of Figs. 3(a) and 3(b) for 1-cm long devices. Similar to Fig. 4(b), the propagation loss was not included in Fig. 6(b) to emphasize that it is the only loss mechanism in the present approach. When propagation loss is included, both type 1 and type 2 reflection-mode devices offer identical true time delays in the range of 51 to 276 ps (i.e., a tunability of 225 ps) when the tunability bit-rate product is maximized at ~5.2.

The performance of the cascaded reflection-mode system is presented in Fig. 7. The system's maximum possible value for tunability-bit-rate product is significantly higher (44.3) than the non-cascaded devices. Also, delay-bit-rate product is impressively high (75.3). The corresponding time delay tuning range is from 87 to 212 ps at this operating condition. As discussed later, by trading off some of the tunability-bit-rate product, higher delay and tunability can be achieved.

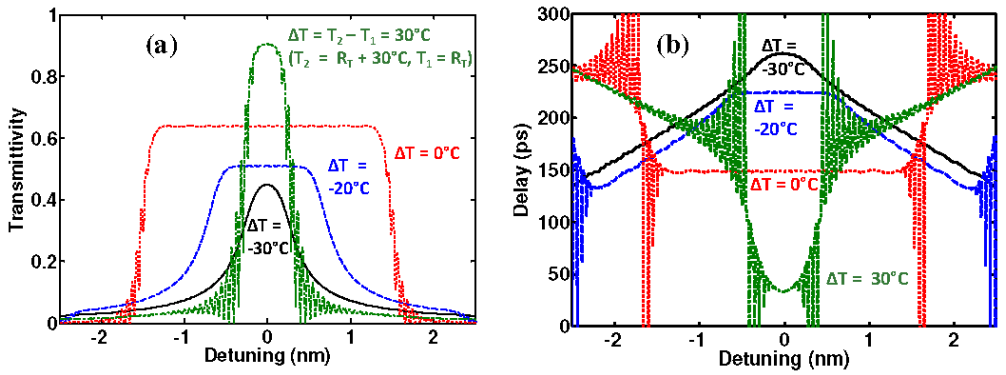

Fig. 7. (a) Transmittivity of the cascaded systems in Fig. 3(e) or (f) based on reflection-mode gratings; (b) Delay spectra of the same systems for various $\Delta T = T_2 - T_1$ (temperature difference of grating 1 and grating 2) around a center wavelength of 1,550 nm.

Figure 8 plots the maximum attainable bit rate and delay versus ΔT for the cascaded devices and compares them with the performance of 1-cm-long single-grating non-cascaded devices. Figure 8(a) is for the reflection-mode devices and Fig. 8(b) is for the transmission-mode devices. In all cases, the temperatures of the gratings vary from R_T to a maximum of R_T + 30°C. Table 1 summarizes the key figures of merits of all of the four studied devices. For the same size, the reflection-mode cascaded complementary delay line outperforms all the other devices in terms of bit rate (355 Gb/s), delay-bit-rate product (75.3) at the mentioned maximum tunability-bit-rate product of 44.3. When the tunability-bit-rate product is maximized for the non-cascaded reflection-mode device a higher delay of 276 ps and a higher tunability of 225 ps can be achieved but the bit rate will be much lower (23.3 Gb/s).

Figure 8 suggests that as ΔT varies for all types of studied devices, so does the limit on bit rate and the delay. This is in contrast to CROWs where bit rate remains constant as ΔT varies [5]. This might imply that since the bit rate changes with temperature in the proposed devices, the device cannot operate at a fixed bit rate and hence they are useless! However, it must be emphasized that the values in Fig. 8 are the maximum attainable bit rate and the devices can always operate at a lower bit rate and with the same delay. So, as long as the attainable delay for a certain operating bit rate is acceptable for a certain fixed bit rate, the devices can function properly. In other words, the only limitation imposed in the performance of the devices is a tradeoff between maximum bit rate and time delay/tunability. For example, at an operation bit rate of 90 Gb/s or lower, a large delay/tunability of 276/225 ps is possible in the reflection-mode cascaded devices. If the operation bit rate is increased to 355 Gb/s, then the delay/tunability limit will be reduced to 212/125 ps. High bit rate operation can be performed at the cost of lower delay and lower tunability.

#168100 - $15.00 USD Received 17 May 2012; revised 4 Aug 2012; accepted 5 Aug 2012; published 15 Aug 2012

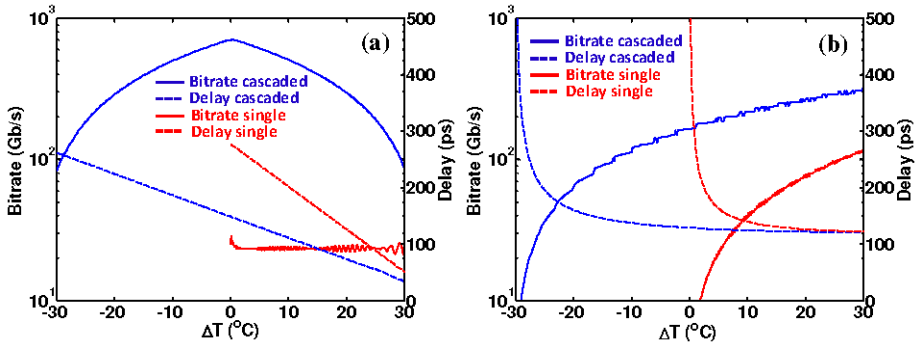

Fig. 8. The maximum attainable bit rate and delay versus $\Delta T = T_2 - T_1$ for the cascaded devices and their comparison with non-cascaded grating waveguides of the same total length ($\Delta T = T - R_T$ in these cases): (a) Reflection-mode devices and (b) Transmission mode devices.

The fundamental limit on loss per time delay (expressed in dB/ns) of any type of guided photonic delay line is $\alpha_T = \alpha c/n_g$, where α is the linear propagation loss, n_g is the group index, and c is the speed of light in vacuum. Indeed, even though slowing the light using gratings, PhCs, CROWs, etc., increases the propagation time (delay) via the enhancement of n_g, the effective propagation length of photons increases by the same factor too. Thus, α_T is independent of enhancement of n_g. The fundamental limit of α_T clearly applies to the case of standard waveguide delay lines. All other types of delay lines, including the present devices, however, suffer from one or more loss mechanisms. For example in the case of CROW-based delay lines, the directional coupling loss between adjacent ring resonators is a significant additional contributor to the overall loss [5]. In the case of PhC waveguide delay lines, the high reflection loss close to the band edge (which scales as n_g^2 [13]) is an additional significant factor. One advantage of the proposed devices is that, because of the employed optimized apodized grating waveguides, there is no grating-induced reflection loss in the transmission operation mode and no transmission loss in the reflection operation mode (see Fig. 4(b) and Fig. 6(b)). There are, however, two other contributors to propagation loss for the present devices. They are the radiation loss of the gratings and scattering from etched sidewalls. The former is due to mode mismatch of adjacent corrugations and the latter is mostly a function of the roughness of etched sidewalls and the effective area of these sidewalls seen by the guided optical mode. Nonetheless, grating waveguides with propagation losses as low as 1.5 dB/cm have been reported [14]. Based on this experimental value, a loss per time delay of 5.3 dB/ns can be predicted for the proposed devices. As a comparison in Table 1 suggests, this expected loss per time delay is far lower than other existing schemes and hence a tunable delay line that compromises between loss and size is achievable.

Table 1. Comparison of the State-of-the-Art Silicon Delay Line Techniques

Device Type	Loss dB/ns	Delay (ps)	Bit rate (Gb/s)	Delay × Bit rate	Tunability† (ps)	Tunability × Bit rate
Waveguide	2.4	124	>1000	>124	~0	~0
CROW [5]	60	89	100	8.9	89	8.9
SCISSOR [6]	34	135	10 (GHz)	1.3	135	1.3
PhC [18]	160	50	10	0.5	33	0.33
Present work:						
Single trans.	5.3	210	11	2.3	90	1
Cascaded trans.	5.3	203	30	6.1	93	2.8
Single refl.	5.3	276	23.3	6.3	225	5.2
Cascaded refl.	5.3	212	355	75.3	125	44.3

† Tunability at fixed wavelength.

It is finally mentioned that faster tuning can be achieved if electrooptic effect (via *p-n* junction diodes) is employed [12] instead of the discussed thermooptic effect. However, this

#168100 - $15.00 USD Received 17 May 2012; revised 4 Aug 2012; accepted 5 Aug 2012; published 15 Aug 2012

faster tuning comes at the expense of extra loss due to the free-carrier absorption in the forward-biased diodes. Our previous work [12], which reports on electrooptic tuning in non-cascaded devices, shows that a loss of < 10 dB is expected for a tunability of ~40 ps, which is much higher than the loss associated with thermo-optic tuning presented here.

4. Conclusions

In summary, a novel class of photonic delay line that comprise two cascaded apodized grating waveguides with complementary (positively and negatively modulated) index profiles for dispersion compensation is proposed. Table 1 summarizes the performance of the studied devices and compares them with the state-of-the-art technologies. It is emphasized that the values for the present work are obtained under the condition of maximum tunability-bit-rate product. The loss values for 1-cm long micron-size spiral waveguides are based on assuming 0.3 dB/cm propagation loss [19]. It is evident that for tunable delay lines, the present reflection-mode cascaded devices have extremely high performance in terms of bit rate (355 Gb/s), delay-bit-rate product (75.3) and tunability-bit-rate product (44.3). The non-cascaded reflection-mode device outperforms all the other devices in terms of delay (276 ps) and tunability (225 ps) but at a lower bit rate of 23.3 Gb/s. Meanwhile, reasonably high performance can be achieved in the transmission-mode cascaded devices which require a simpler architecture (compare Fig. 1(d) to Figs. 3(d) and 3(e)).

Acknowledgment

The work is being supported by the United States' National Science Foundation under the Award Number 1128208.

#168100 - $15.00 USD Received 17 May 2012; revised 4 Aug 2012; accepted 5 Aug 2012; published 15 Aug 2012